Surface-assisted coordination chemistry and self-assembly†

Nian Lin,*[a] Sebastian Stepanow,[a] Franck Vidal,[a] Klaus Kern,[a,b] Mohammad S. Alam,[c] Stefan Strömsdörfer,[c] Viacheslav Dremov,[c] Paul Müller,[c] Aitor Landa[d] and Mario Ruben*[d]

Received 7th November 2005, Accepted 20th December 2005
First published as an Advance Article on the web 8th May 2006
DOI: 10.1039/b515728e

This article discusses different approaches to build up supramolecular nanoarchitectures on surfaces, which were simultaneously investigated by scanning tunneling microscopy (STM) on the single-molecule level. Following this general road map, first, the hydrogen-bonding guided self-assembly of two different, structural-equivalent molecular building blocks, azobenzene dicarboxylic acid and stilbene dicarboxylic acid, was studied. Secondly, the coordination chemistry of the same building blocks, now acting as ligands in metal coordination reactions, towards co-sublimed Fe atoms was studied under near surface-conditions. Extended two-dimensional tetragonal network formation with unusual $Fe_2L_{4/2}$-dimers at the crossing points was observed on copper surfaces. Complementary to the first two experiments, a two-step approach based on the solution-based self-assembly of square-like tetranuclear complexes of the M_4L_4-type with subsequent deposition on graphite surfaces was investigated. One- and two-dimensional arrangements as well as single molecules of the M_4L_4-complexes could be observed. Moreover, the local electronic properties of a single M_4L_4-complexes could be probed with submolecular resolution by means of scanning tunnelling spectroscopy (STS).

1 Introduction

(Supra)molecular nanostructures have recently attracted rising interest in view of their potential to host tuneable functionalities (*e.g.* electronic, magnetic, optic *etc.*), which might be become accessible within the few-nanometre regime.[1] Towards this ambitious goal, the combination of controlled generation of molecular nanostructures under near-surface conditions using self-assembly concepts (*e.g.* reversible hydrogen- and coordinative bond formation) with the concomitant application of scanning tunnelling microscopy (STM) and spectroscopy (STS) techniques seems to be a promising and straightforward concept.[2]

Due to its central role in the bottom-up strategy to fabricate nanostructures, self-assembly techniques have recently gained extensive interest.[3] Such techniques offer opportunities for the design of nanostructures by the use of constituting components with appropriate intrinsic structural and functional information. Such components can be active building blocks bearing a specific manipulable property, a so called functionality, while at the same time they have to be capable to self-assemble to higher-order supramolecular structures *via* specific molecular interactions. The used interactions are generally relatively weak in terms of binding energy and range from van der Waals and electrostatic forces over π–π- and hydrogen-bonding to coordination bond formation processes. Reversibility of the processes is crucial for successful formation, since it enables the constituents to move along an assemble path reaching the most energetically stable supramolecular configuration. It is also the procedural base of such phenomena as self-healing or self-adaptation. In general, the final topology of such an assembly is determined by the structural information stored in its constituents and the way how this information is read out taking advantage of the electronic selectivity and the spatial directionality in bond formation and interaction.

Since most of the approaches to exploit the physical properties of supramolecular nanostructures demand a direct spatial and very often electronic addressing, controlled arrangements of the components exhibiting a high degree of periodicity in two dimensions (2D) are required. Driven by this need, the investigation of self-assembly processes under assistance of the underlying surface is an approach of special interest.[4] Since the deposition of bulk-assembled bricks might alter the structural and physical (bulk) properties by inevitably occurring molecule–surface interactions, the understanding of "surface-assisted" self-assembly opens a way to direct molecular level control of the positioning and addressing of surface-adapted functional units. The character of the interactions of the molecules with the substrate is worth to be investigated by itself and further insight might give access to alternative, maybe purely surface-based ways of exploitation of real single-molecule information.[5]

Based on this conceptual guide, three general approaches towards self-assembled supramolecular nanostructures at surfaces will be discussed in this article (see Fig. 1): (A) The one-step surface-assisted self-assembly of organic nanostructures steered by hydrogen-bond formation. Thereby, the hydrogen-bond guided self-assembly of two dicarboxylic acid derivates, namely 4′,4″ *trans*-ethene-1,2-diyl-bisbenzoic acid (**1**), and 4,4′-azobenzene

[a]*Max-Planck-Institut für Festkörperforschung, Heisenbergstrasse 1, D-70569, Stuttgart, Germany. E-mail: n.lin@fkf.mpg.de; Fax: 49 7116891662; Tel: 49 7116891617*
[b]*Institut de Physique des Nanostructures, Ecole Polytechnique Fédérale de Lausanne, CH-1015, Lausanne, Switzerland*
[c]*Physikalisches Institut III, Universität Erlangen-Nürnberg, Erwin Rommel-Str. 1, 91058, Erlangen, Germany*
[d]*Institut für Nanotechnologie, Forschungszentrum Karlsruhe GmbH, PF 3640, D-76021, Karlsruhe, Germany. E-mail: Mario.Ruben@int.fzk.de; Fax: +497247826434; Tel: +497247826781*
† Based on the presentation given at Dalton Discussion No. 9, 19–21st April 2006, Hulme Hall, Manchester, UK.

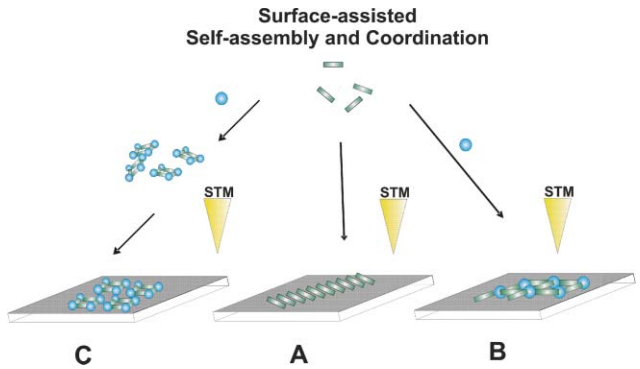

Fig. 1 Schematic representation of three different approaches to generate supramolecular nanostructures on surfaces (rods: tailored organic molecules, spheres: metal ions). (A) Surface-assisted self-assembly by hydrogen-bond formation; (B) surface-assisted self-assembly by coordination bond formation, and (C) the surface deposition of previously in the bulk self-assembled supramolecular architectures.

dicarboxylic acids, (**2**) on a copper (100) surface will be investigated (Scheme 1). The coordination chemistry of the same organic molecules **1** and **2**, now acting as ligands to Fe ions through their deprotonated carboxylate groups, will be studied in approach (B). Approach (C) consist of two separated steps with (i) pre-assembling and (ii) deposition of supramolecular metal complexes onto surfaces (Fig. 1). In detail, the grid-like supramolecular complex $[M_4(\mathbf{3})_4](BF_4)_8$ (**4**) was assembled in bulk and than deposited onto graphite surfaces (see Fig. 1 and Scheme 1). Since the grid-like complex **4** is not sublimable, a solution-based deposition from acetonitrile was applied. Complexes of the $[M_4(L)_4]$-grid-type are known to exhibit very interesting optical, electronic and magnetic properties.[6]

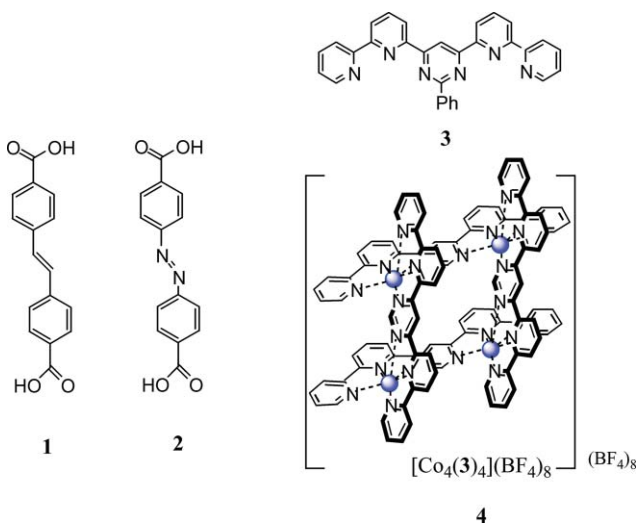

Scheme 1

Generally, all structural characteristics of the supramolecular assemblies were elucidated by STM investigations. In addition, the local electronic properties of the complex **4** were addressed on the submolecular level by STS measurements.

In this article, we describe a general road map proposing three different routes towards the controlled generation of 2D, highly-ordered functional molecular nanostructures at different surfaces. Additionally, we introduce an approach towards the investigation and manipulation of molecular functionalities at the single-molecule level.

2 Syntheses and characterization

The organic molecules were purchased (**1**) or synthesized following literature procedures (**2**).[7] Both compounds were purified by a two-fold sublimation before used in the experiments. Ligand **3** and the complex $[Co^{II}_4(\mathbf{3})_4](BF_4)_8$ (**4**) were synthesized as described before.[8]

STM measurements on Cu(100)

The preparation and characterization of the supramolecular assembly on surfaces from molecular building blocks were carried out in a ultra-high vacuum (UHV) apparatus with a base pressure of $\sim 3 \times 10^{-10}$ mbar (Fig. 2).[9] The Cu(100) surface was cleaned by repeated cycles of Ar^+ sputtering and annealing at 800 K, which leads to an atomically flat and clean surface. Compounds **1** and **2** were deposited onto the substrate held at 298 K by organic molecular beam epitaxy (OMBE) from Knudsen-cell type evaporators at temperatures of 500 and 505 K, respectively. To facilitate the self-assembly processes, we used coverage below monolayer saturation and annealed the sample to 400 K. To invoke metal coordination, Fe atoms were subsequently evaporated onto the molecular adlayers using an e-beam heating evaporator. Samples were annealed after deposition at 450 K for 5 min to increase the adsorbates' mobility and reactivity and thus to obtain well-ordered structures. The sample was then cooled down to room temperature and transferred to a scanning tunneling microscope in the same vacuum system for structural characterization. The STM measurements were performed in the constant current mode at room temperature, with 0.5 V bias voltage and 1.0 nA tunneling current. The resolution of the dog bone like molecules in the STM data as anisotropic protrusions, ~1 nm in length, reveals that the two species adsorb in a flat-lying geometry, in agreement with the bonding of other species containing aromatic ligands adsorbed at metal surfaces in ultra-high vacuum conditions.[10]

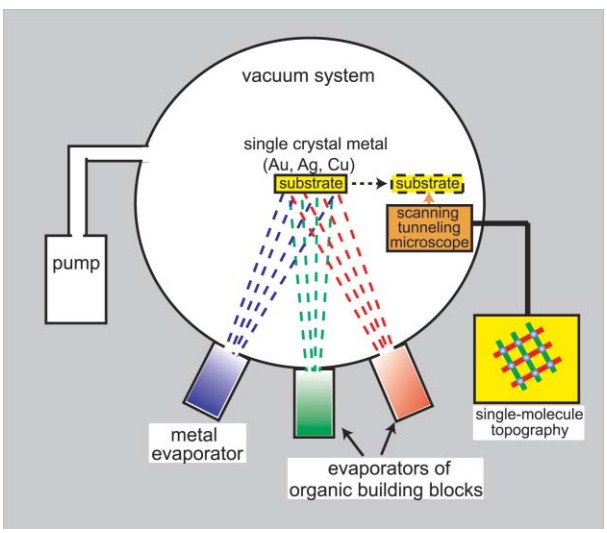

Fig. 2 Schematic drawing of the experimental setup for direct preparation and characterization of 2D supramolecular assemblies on metallic surfaces.

STM measurements on graphite

All measurements on graphite were carried out under ambient conditions with a home built low drift STM head equipped with commercially available low current control electronics (RHK technology). A droplet of a solution of the complex **4** (typically 10^{-9} M) was deposited and was let the droplet run down the graphite (HOPG) surface. Tunneling currents between 5 and 200 pA bias voltage of ±50 to ±500 mV were employed in the STM measurements. The scan frequency was varied between 2 and 5 Hz and the resolution was set to 256 × 256 points for topography and to 128 × 128 in the STS measurements. In the STS mode, current–voltage (*I*–*V*) curves were taken simultaneously with a constant-current STM image with the interrupted-feedback loop technique. The scan range of voltages was typically from −1.5 to 0.1 V relative to the tip potential for approximately 100 discrete voltage steps. Typically, tunneling resistances of the order of 1 GΩ were set. Mechanically cut Pt–Ir (90/10) tips from wires with a diameter of 0.25 mm were used. Fig. 7 and 8 were generated using the program WSxM (Nanotec Electrónica, Madrid).

3 Results and discussion

3.1 Surface-assisted self-assembly by hydrogen bonding

On Cu(100) surface, molecule **1** assembles readily into ordered 2-D supramolecular structures, which have typically domain sizes of about 10 nm (Fig. 3). The domains are almost defect-free and nearly all molecules of **1** are incorporated into domains of different sizes. The self-assembly of **1** accounts for a square-like motif, in which each molecule is perpendicularly disposed with respect to its neighboring molecule. Hydrogen-bonds between the oxygen atoms of a deprotonated carboxylato group[11] and the hydrogen atoms of the ethenylene bond of the neighbors form the extended network. The corresponding unit cell (*cf.* the white squares in Fig. 3) is oriented 36° clockwise off the [001] direction. Moreover, a second phase, whose unit cell is oriented 36° counterclockwise off the substrate [001] direction, was also observed as shown in Fig. 3.

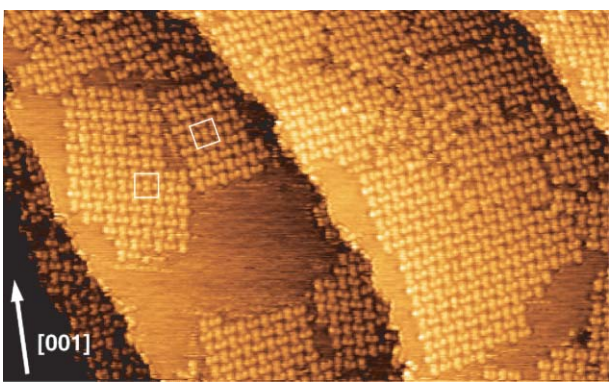

Fig. 3 STM image of the hydrogen-bond driven self-assembled supramolecular domains of molecule **1** on a Cu(100) surface. The squares indicate the unit cells within the two enantiomerically resolved mirror domains (image size: 55 × 34 nm).

The molecule **1** possesses a two-dimensional (2D) pro-chirality, which is deconvoluted if the molecules are confined on the surface. Over the last years, several 2D chiral molecular systems have been studied in contact with surfaces.[12] In particular, it has been shown in STM experiments that chiral recognition and resolution processes can be initiated by the self-assembly of racemic mixtures of molecular species exhibiting 2D prochirality. In the case of molecule **1**, the hydrogen bond formation among the surface-adsorbed molecules of **1** drives the chiral resolution process rendering enantiomerically pure homochiral phases. Further details describing this process are given elsewhere.[13]

The compound **2**, in which the central double bond is replaced by a diazo group, forms also supramolecular domains on Cu(100) surface under the given conditions (*cf.* ovals in Fig. 4). In contrast to **1**, the domains consist internally of the molecules, which are now organized by hydrogen bonding interactions in a brick-wall like pattern. However, in addition to the observed domains, a large fraction of molecules of **2** is also involved in the formation of short chains or other, less defined small aggregates (Fig. 4). Obviously, the long-range ordering during the domain formation is less efficient for molecule **2**. A closer STM analysis elucidates that the brick-wall pattern relies on a different hydrogen-bonding pattern as observed in the case of molecule **1**: The hydrogen bond formation occurs exclusively between the oxygen atoms of deprotonated carboxylato groups and phenyl hydrogen atoms. Nevertheless, 2D chiral deconvolution into homochiral phases with mirror symmetry was observed for molecule **2**, too.[13]

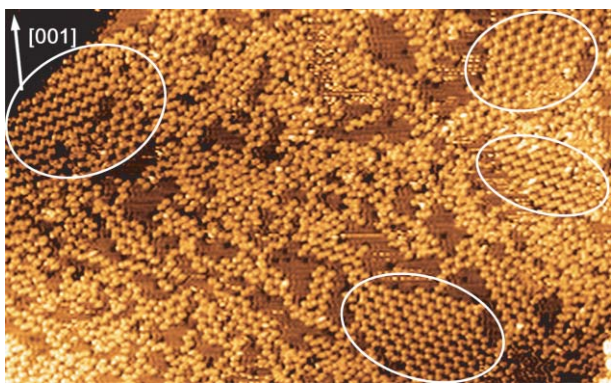

Fig. 4 STM image of the different types of hydrogen-bonding domains of molecule **2** on Cu(100). The ovals indicate highly-ordered brick-wall domains, in the left-upper corner, the appearance of two mirror-phases is shown (image size: 55 × 34 nm).

Both molecules **1** and **2** employ deprotonated carboxylato moieties as hydrogen-bond acceptors, while the hydrogen-bond donors vary between ethenyl protons in **1** and phenyl protons in **2**. The slight variation in the atomic identity of the molecules is so reproduced in different internal structures of the domains. Hence a clear correlation between the fine-structure of the molecular building blocks and the organizational topology can be drawn, which may provide a rational route to design supramolecular surface structures by the use of suited molecular bricks.

3.2 Surface-assisted metal coordination

Subsequent sublimation of Fe atoms onto the respective hydrogen-bound supramolecular assemblies of **1** or **2** leads to a complete

reorganization of the organic phases. High-resolution STM topography images allow determining unambiguously the formation of infinite tetragonal networks in both cases. Representative STM data of the Fe-coordinated networks of **1** are shown in Fig. 5. Since the individual iron atoms are clearly resolved, it can be concluded that the network is interconnected at the crossing points by $Fe_2(\mathbf{1})_{4/2}$-nodes. The so observed Fe_2-dimers in the cross positions of the network deserve some interest due to their coordination characteristics: Two Fe centers are surrounded by two sets of differently coordinating carboxylic groups; two of them are in a μ_2-bridging mode and two bind in an apparently monodentate mode. However, since the resolution limits of the present STM data do not allow a clear distinction between the mono- and bidentate coordination modes of the two chelating carboxylic groups, a conclusive determination of the coordination geometry is not unambiguously possible. But coordination environment might be interpreted at the best by four quadratic-planar disposed oxygen atoms around each Fe-centre. To our knowledge, such Fe_2-dimers with quadratic planar coordination are so far unknown in bulk materials. However, on surfaces, the coordination characteristics of metal ions might be strongly influenced and partially distorted by templating effects by the underlying crystal lattice of the substrate. On the other hand, the Fe–O bond distances estimated from the STM data are close to those known from bulk materials (d(Fe–O) ≈ 2.0 Å). Thus, the metal centers of the dimers are held in a metal-metal distance of about d(Fe–Fe) ≈ 4.2 Å.

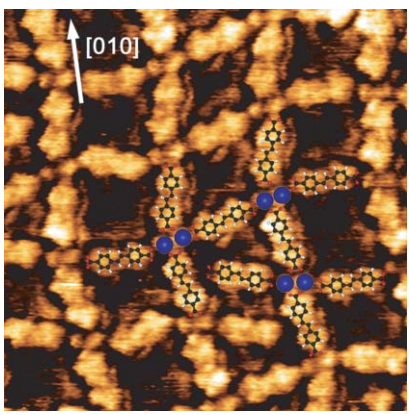

Fig. 5 High-resolution STM topography of Fe-coordinated open network phase of **1** (image size: 8.4 × 8.4 nm). The white arrow is the substrate [011] orientation. A tentative model is drawn overlaying the data. Fe atoms are represented by blue spheres.

Sublimation of Fe atoms onto the brick-wall 2D domains of compound **2** renders likewise an infinite tetragonal network with structural characteristics, *e.g.*, network topologies and the dimeric $Fe_2(\mathbf{2})_{4/2}$ nodes, very similar to those described above for the system **1**/Fe (Fig. 6).

In comparison with earlier work on surface-assisted Fe-carboxylate coordination systems mainly using linear organic building blocks,[14] the networks of **1** and **2** show the some particular features: (i) the size of single-domain networks formed by both, **1** and **2**, is relatively small, *i.e.*, most of the observed single domains do not exceed 10 nm in size; (ii) the formed structures show relatively many structural defects (see Fig. 5); (iii) the 2D cavities of the networks have a variety of geometries, and (iv) the

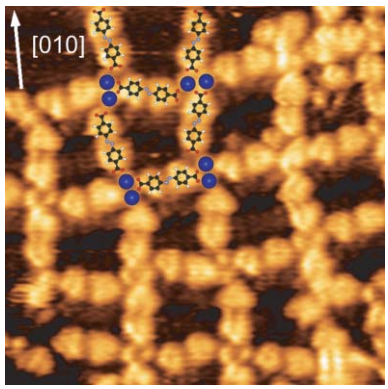

Fig. 6 High-resolution STM topography of Fe-coordinated open network phase of **2** (image size: 8.4 × 8.4 nm). The white arrow is the substrate [011] orientation. A tentative model is drawn overlaying the data. Fe atoms are represented by blue spheres.

axial orientation of iron pairs is arbitrary, lacking of any regular pattern observed in other systems. These differences, especially the restricted domain size, can be attributed to the lowered symmetry of **1** and **2** (compared with the linear ligands). The presence of 2D enantiomeric building blocks, which are randomly arranged (in contrast to the chirally-resolved hydrogen-bond structures), may cause that the networks cannot develop into a perfect periodic structure that is commensurate to the substrate lattice. So the molecules and Fe atoms start to occupy non-equivalent sites of the substrate lattice which causes additional energy costs. As a consequence, the long-range translation of the coordination binding nodes in two directions is hindered and structural defects appear more frequently.

The preliminary discussion of the electronic properties (*e.g.* oxidation and spin states) of the metal centers within the coordination network has to take into consideration rather unusual contributions like the electronic coupling of the metal centers to the substrate or possible counterbalancing of the charges of the assembled molecular structures by mirror charges within the upper layers of the metallic substrate. But looking at the distinct $M_2L_{4/2}$-stoichiometry of the dimeric Fe_2-nodes, it seems reasonable to reckon that the principle of electro-neutrality is also persisting under near-surface conditions. Such a view would lead to the definition of two Fe(II) ions surrounded by four deprotonated, negatively charged carboxylic groups. The formation of electro-neutral 4+/4− units will depend critically on the smoothness of the deprotonation reaction. Alternatively to the spontaneous deprotonation of carboxylic acid groups on copper surfaces,[11] a redox reaction involving the reduction of four carboxylic protons under simultaneous oxidation of the two iron(0) centers might be considered, too. The gaseous hydrogen could easily migrate into the UHV environment so favoring the accomplishment of the redox reaction. Experiments (*e.g.* X-ray absorption spectroscopy and X-ray magnetic circular dichroism) to determine the oxidation- and coordination numbers as well as the magnetic behavior of the involved Fe-centers are under way.

3.3 Surface-deposition of pre-assembled complexes

In order to gain better control over so crucial issues as coordination number and oxidation state of central atoms of our

complexes also under near surface conditions, we have decided to synthesize grid-like [2 × 2]-type complexes $[M_4(\mathbf{3})_4]$ $(BF_4)_8$ (**4**) by solution-based self-assembly from ligand molecules **3** and Co(II) ions (Scheme 1). The so-obtained complex **4** was subsequently deposited onto graphite surfaces in a second, separated step. Due to the high charge of the molecule, direct sublimation of the molecules was not possible.

STM studies of densely packed monolayers of $[Co^{II}_4L_4]^{8+}$ grid complexes on graphite had already been reported before.[15,16] In order to study the specific features of the electronic properties at the single-molecule level, we concentrated our work on isolated, free-standing molecules. Related approaches dealing with the investigation of specific functionalities of supramolecular nanostructures on surfaces and under ambient conditions were reviewed recently.[17,18]

Since the structural and electronic information of STM measurements are strongly entangled,[19] the interpretation and analysis of the images of rather complex molecules is not straightforward. However, scanning tunneling spectroscopy (STS) measurements can reveal direct information about the molecular energy levels, especially those which are close to the Fermi level. Functional units of atoms can be distinguished by selective mapping of certain energy regions, provided that their corresponding orbitals are well separated in energy. In general, such STS experiments are carried out under rather rigorous conditions (metallic single crystals, ultra high vacuum conditions and low temperatures) to minimize the coupling of the system with the environment.[20] However, it was also shown that under certain conditions room temperature STM experiments enable to detect local electronic property changes of molecules resulting *e.g.* from intramolecular acceptor–donor,[21a] from intermolecular π–π[21b] or charge transfer interactions.[21c]

Using a home-made STM head optimized for low drift under ambient conditions, high resolution topography mapping could be successfully combined with simultaneous current–voltage characteristics (STS) measurements on single molecules deposited onto graphite surfaces. The investigated samples were prepared by depositing a drop of a solution of $[Co^{II}_4(\mathbf{3})_4]^{8+}$ molecules in acetonitrile (10^{-9} mol l^{-1}) onto the freshly cleaved graphite surface. Different molecular arrangements of Co [2 × 2] grid complexes on the substrate could be observed after repeated scanning with relatively mild tunneling conditions (Fig. 7). At low coverage, the grid complexes got trapped along the step edges of graphite and it was possible to obtain continuous 1D chains of several hundred nanometers lengths (Fig. 7(a)). Increasing the coverage led to 2D arrays of densely packed molecules of **4** (Fig. 7(b)). The ordered 2D structures grow spontaneously starting from single nucleation points, what can be considered as the 2D equivalent of a crystallization process. On further decreasing the coverage, a well ordered distribution of isolated units was found. This distribution was even stable at room temperature, where thermal mobility becomes appreciable and which illustrates the delicate adsorbate–substrate interactions in the system of **4** and graphite.

Fig. 7(c) shows a high-resolution STM image of a single $[Co^{II}_4(\mathbf{3})_4](BF_4)_8$ complex. The image appears as a bright uniform spot with a cross-section of about 1.7 nm surrounded by a less defined halo, which can be caused by contributions from the BF_4-anions and solvent molecules, and fits to the molecular size extracted from single-crystal X-ray diffraction studies (1.65 nm).[8] Additionally, a quadratic set of slightly brighter spots can be observed on top of the structure anticipating the positions of the cornerstone metal ions. Besides these faint features, as expected, STM topography cannot provide any further information on the intramolecular structure.

In order to investigate the electronic properties of the deposited $[Co^{II}_4(\mathbf{3})_4](BF_4)_8$ molecules, we have applied current imaging tunneling spectroscopy (CITS) techniques to the molecule–substrate system. CITS techniques have been developed for scanning tunneling spectroscopy (STS) of a sample surface and consist in the recording of current–voltage (I–V) characteristics at every pixel position of the topography map maintaining a constant tip to surface distance.[22–24] The I–V data set can be sorted such that it provides both a height (topography) map, taken at constant current, and several tens of current (CITS) maps, taken at constant voltage. The current contrast changes significantly when at certain bias voltages new molecular energy levels come into play.

STS techniques were so successfully applied to a [2 × 2] Co^{II}_4 grid-type complex, although the investigations were so far restricted to negative sample-to-tip bias voltages, *i.e.* to the spectroscopy of occupied levels. Whereas, the topographic image, Fig. 7(c), presents a rather featureless structure with a diameter of approximately 1.7 nm, the STS 3D current maps, Fig. 8, let

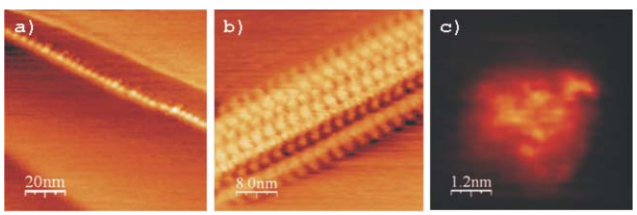

Fig. 7 STM images of $[Co^{II}_4(\mathbf{3})_4](BF_4)_8$ (**4**) grid-like complexes deposited onto a graphite surface showing (a) the complexes aligned along graphite steps into 1D chains; (b) a 2D crystal, and (c) an isolated molecule formed from molecules of **4**.

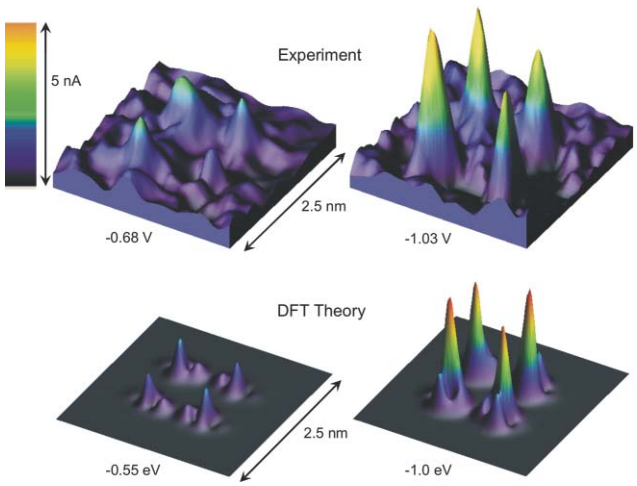

Fig. 8 (Top) Set of STS (CITS) 3D current images representing a single $[Co^{II}_4(\mathbf{3})_4](BF_4)_8$, **4** at two different tunnel biases. bottom) DFT calculated electron density maps calculated within both energy windows.[25] The left one covers the range between the Fermi energy E_F and the HOMO (−0.55 eV), while the right one covers the full range between E_F and all states exhibiting 3d character (−1.0 eV).

emerge a quadratic array of four sharp peaks representing clear maxima of the tunneling current. The background current arising from the graphite surface was subtracted. The peak array has a side length of approximately 0.7 nm. This result is in accord to the distance between two neighboring Co ions determined by X-ray crystallography[8] and with the data obtained in DFT calculations (Fig. 8, lower row).[25] The clear four-peak structure is a consequence of the fact that the highest occupied states of the molecule are exclusively composed of Co 3d states. Therefore, the four metal ions can be mapped without any influence from the rest of the ligands.

4 Conclusions

In this article, we introduce a general road map exhibiting three different routes of controlled generation of 2D highly-ordered functional molecular nanostructures and their surface investigation at the single-molecule level.

In the first route, the hydrogen bond formation capability of two molecular bricks, **1** and **2**, was exploited to assemble them on Cu(100) surfaces into supramolecular domains with distinct internal structure. Although being structurally very similar, the two molecules rendered different supramolecular motifs. Structure-evolving forces are hydrogen bonding interactions between the deprotonated carboxylate groups with either phenyl protons (in the case of **2**) or with ethenyl protons (in the case of **1**). The surface-assisted self-assembly leads to the deconvolution of the intrinsic molecular 2D prochirality of **1** and **2** into homo-chiral supramolecular domains.

In the second route, the surface-assisted coordination chemistry approach, the supramolecular assemblies on the Cu(100) surface of **1** and **2** were completely reorganized by the co-sublimation of Fe metal atoms. The coordination of the metal atoms through the deprotonated carboxylato groups yielded infinite tetragonal network structures with internal open cavities of variable topography. The node positions of the network are formed by $Fe_2L_{4/2}$ dimers, in which the metal centers are coordinated in a quadratic planar fashion by four carboxylato groups, respectively. Such coordination motif is unprecedented for iron centers under bulk conditions. Ongoing investigations will have to determine the characteristics of the metal centres, such as oxidation and coordination number as well as the structural and electronic impact of the underlying metallic surface.

In order to improve the control of the coordination environment of the metal centres, we have pre-assembled a $Co^{II}{}_4L_4$ grid-type complex **4** in solution and deposited it subsequently onto graphite surfaces. There, assemblies of the grid-type complexes were imaged by STM techniques applied under ambient conditions. At low coverage, the complexes were shown to align preferably with the step edges of the graphite surface. By this way, it was possible to generate several free-standing 0D, 1D and 2D assemblies. Room-temperature STS measurements on isolated single complexes allowed the direct addressing the metal centers buried within the supramolecular architectures with submolecular resolution.

The herein introduced road map towards the surface-assisted self-assembly and coordination chemistry under near-surface conditions might constitute part of the future tool kit needed to put into reality steered built-up and controlled manipulation of functional interfaces and operational surfaces.

Acknowledgements

This work was generously supported by the EC-FP VI STREP "BIOMACH" (NMP4-CT-2003-505-487) and by the ESF-EUROCORES-SONS project "FunSMARTs".

References

1 J.-M. Lehn, *Supramolecular Chemistry. Concepts and Perspectives*, VCH, Weinheim, 1995, ch. 9 and p. 200; J.-M. Lehn, *Science*, 2002, **295**, 2400–2403; J.-M. Lehn, *Proc. Natl. Acad. Sci. USA*, 2002, **99**, 4763–4768.
2 M. Ruben, *Angew. Chem., Int. Ed.*, 2005, **44**, 1594–1596.
3 See: A. Schlüter (Editor), Functional Molecular Nanostructures, *Top. Curr. Chem.*, 2005, **245**, and references therein.
4 J. V. Barth, G. Costantini and K. Kern, *Nature*, 2005, **437**, 671, and references therein.
5 Barth, J. Weckesser, C. Cai, P. Günter, L. Bürgi, O. Jeandupeux and K. Kern, *Angew. Chem., Int. Ed.*, 2000, **39**, 1230; H. Spillmann, A. Dmitriev, N. Lin, P. Messina, J. V. Barth and K. Kern, *J. Am. Chem. Soc.*, 2003, **125**, 10725; J. A. Theobald, N. S. Oxtoby, M. A. Phillips, N. R. Champness and P. H. Beton, *Nature*, 2003, **424**, 1029.
6 Optical: M. Ruben, J.-M. Lehn and G. Vaughan, *Chem. Commun.*, 2003, 1338; magnetic: O. Waldmann, J. Hassmann, P. Müller, G. S. Hanan, D. Volkmer, U. S. Schubert and J.-M. Lehn, *Phys. Rev. Lett.*, 1997, **78**, 3390; E. Breuning, M. Ruben, J.-M. Lehn, F. Renz, Y. Garcia, V. Ksenofontov, P. Gütlich, E. Wegelius and K. Rissanen, *Angew. Chem., Int. Ed.*, 2000, **39**, 2504–2507; M. Ruben, E. Breuning, J.-M. Lehn, V. Ksenofontov, F. Renz, P. Gütlich and G. Vaughan, *Chem. Eur. J.*, 2003, **9**, 4422–4429; M. Ruben, U. Ziener, J.-M. Lehn, V. Ksenofontov, P. Gütlich and G. B. M. Vaughan, *Chem. Eur. J.*, 2005, **11**, 94–100; electronic: M. Ruben, E. Breuning, J.-P. Gisselbrecht and J.-M. Lehn, *Angew. Chem., Int. Ed.*, 2000, **39**, 4139–4142; D. M. Bassani, J.-M. Lehn, S. Serroni, F. Puntoriero and S. Campagna, *Chem. Eur. J.*, 2003, **9**, 5936–5946.
7 A. I. Khalaf, A. R. Pitt, M. Scobie, C. J. Suckling, J. Urwin, R. D. Waigh, R. V. Fishleigh, S. C. Young and W. A. Wylie, *Tetrahedron*, 2000, **56**, 5225–5228.
8 M. Ruben, E. Breuning, M. Barboiu, J.-P. Gisselbrecht and J.-M. Lehn, *Chem. Eur. J.*, 2003, **9**, 291–299.
9 A. Dmitriev, N. Lin, J. Weckesser, J. V. Barth and K. Kern, *J. Phys. Chem. B*, 2002, **106**, 6907.
10 J. Weckesser, J. V. Barth and K. Kern, *J. Chem. Phys.*, 1999, **110**, 5351; P. Sautet, *Chem. Rev.*, 1997, **97**, 1097; P. H. Lippel, R. J. Wilson, M. D. Miller, Ch. Woell and S. Chiang, *Phys. Rev. Lett.*, 1989, **62**, 171; F. Vidal, E. Delvigne, S. Stepanow, N. Lin, J. V. Barth and K. Kern, *J. Am. Chem. Soc.*, 2005, **127**, 10101.
11 C. C. Perry, S. Haq, B. G. Frederick and N. V. Richardson, *Surf. Sci.*, 1998, **409**, 512; N. Lin, A. Dmitriev, J. Weckesser, J. V. Barth and K. Kern, *Angew. Chem., Int. Ed.*, 2002, **41**, 4779; S. Stepanow, T. Strunskus, M. Lingenfelder, A. Dmitriev, H. Spillmann, N. Lin, J. V. Barth, Ch. Wöll and K. Kern, *J. Phys. Chem.*, 2004, **108**, 19392.
12 S. M. Barlow and R. Raval, *Surf. Sci. Rep.*, 2003, **50**, 201–341, and references therein; V. Humblot, S. M. Barlow and R. Raval, *Prog. Surf. Sci.*, 2004, **76**, 1, and references therein.
13 S. Stepanow, N. Lin, F. Vidal, A. Landa, M. Ruben, J. V. Barth and K. Kern, *Nano Lett.*, 2005, **5**, 901–904.
14 A. Dmitriev, H. Spillmann, N. Lin, J. V. Barth and K. Kern, *Angew. Chem., Int. Ed.*, 2003, **42**, 2670; S. Stepanow, M. Lingenfelder, A. Dmitriev, H. Spillmann, E. Delvigne, N. Lin, X. Deng, C. Cai, J. V. Barth and K. Kern, *Nat. Mater.*, 2004, **3**, 229; M. A. Lingenfelder, H. Spillmann, A. Dmitriev, S. Stepanow, N. Lin, J. V. Barth and K. Kern, *Chem. Eur. J.*, 2004, **10**, 1913; N. Lin, S. Stepanow, F. Vidal, J. V. Barth and K. Kern, *Chem. Commun*, 2005, 1681.
15 A. Semenov, J. P. Spatz, J.-M. Lehn, C. H. Weidl, U. S. Schubert and M. Möller, *Appl. Surf. Sci.*, 1999, **144–145**, 456; A. Semenov, J. P. Spatz, M. Möller, J.-M. Lehn, B. Sell, D. Schubert, C. H. Weidl and U. S. Schubert, *Angew. Chem., Int. Ed.*, 1999, **38**, 2547.
16 U. Ziener, J.-M. Lehn, A. Mourran and M. Möller, *Chem. Eur. J.*, 2002, **8**, 951.

17 S. De Feyter and F. C. De Schryver, *Chem. Soc. Rev.*, 2003, **32**, 139.
18 P. Samorí, *Chem. Soc. Rev.*, 2005, **34**, 551–561.
19 Ó. Paz, I. Brihuega, J. M. Gómez-Rodríguez and J. M. Soler, *Phys. Rev. Lett.*, 2005, **94**, 056103.
20 (*a*) W. Ho, *J. Chem. Phys.*, 2002, **117**, 11033–11061; (*b*) P. Wahl, L. Diekhöner, M. A. Schneider, L. Vitali, G. Wittich and K. Kern, *Phys. Rev. Lett.*, 2004, **93**, 176603.
21 (*a*) A. Miura, Z. Chen, H. Uji-i, S. De Feyter, M. Sdanowska, P. Jonkhejm, A. P. H. J. Schenning, B. Mejer, F. Würthner and F. C. De Schryver, *J. Am. Soc. Chem.*, 2003, **125**, 14968–14969; (*b*) A. Gesquiere, S. De Feyter and F. C. De Schryver, *Nano Lett.*, 2001, **1**, 201–206; (*c*) F. Jäckel, M. D. Watson, K. Müllen and J. P. Rabe, *Phys. Rev. Lett.*, 2004, **92**, 188303.
22 R. J. Hamers, R. M. Tromp and J. E. Demuth, *Phys. Rev. Lett.*, 1986, **56**, 1974.
23 S. Novokmet, M. S. Alam, V. Dremov, F. W. Heinemann, P. Müller and R. Alsfasser, *Angew. Chem., Int. Ed.*, 2005, **44**, 803.
24 A. M. Ako, H. Maid, S. Sperner, S. H. H. Zaidi, R. W. Saalfrank, M. S. Alam, P. Müller and F. W. Heinemann, *Supramol. Chem.*, 2005, **17**, 315.
25 M. S. Alam, S. Strömsdörfer, S. Dremov, P. Müller, J. Kortus, M. Ruben and J.-M. Lehn, *Angew. Chem., Int. Ed.*, 2005, **44**, 7896–7899.

